KSCE Journal of Civil Engineering (2021) 25(8):3075-3083
DOI 10.1007/s12205-021-2130-2

pISSN 1226-7988, eISSN 1976-3808
www.springer.com/12205

Structural Engineering

Layout Optimization of Stiffeners in Heavy-Duty Thin-Plate Box Grider

Hao Zhang[a], Yixiao Qin[a], Jinpeng Gu[a], Haibiao Gao[a], Qianqian Jiao[a], Feng Wang[a], Zhenshan Guo[a], Yangyang Zhang[a], and Chenghong Mi[b]

[a]*College of Mechanical Engineering, Taiyuan University of Science and Technology, Taiyuan 030024, China*
[b]*Xuzhou Construction Machinery Co., Ltd., Xuzhou 221000, China*

ARTICLE HISTORY

Received 30 November 2020
Revised 8 February 2021
Accepted 17 March 2021
Published Online 26 May 2021

KEYWORDS

Bias-rail box girder
Longitudinal stiffening ribs
Transverse diaphragms
Layout optimization
Coupling of structural analysis and optimization

ABSTRACT

The optimization of layout and sizes of the stiffeners in heavy-duty box girder could make this kind of the structure more compact and reasonable, which has certain engineering values. In this study, on the basis of the establishment of parametric finite element model, the function approaching method and gradient search method are combined to form a high-precision optimization algorithm, which makes structural analysis be integrated into the optimization process. The optimization takes the type and location of longitudinal stiffening ribs and the thickness and hole position of transverse diaphragms as design variables, the box girder structural behaviors as constraint conditions, and the total volume as objective function. Finally, the weight is reduced by nearly 7%. More importantly, the new asymmetrical layout of the stiffeners is obtained, the distance between the longitudinal stiffening ribs on the main web and the neutral layer is longer than the distance between the longitudinal stiffening ribs on the secondary web and the neutral layer, and the hole position of transverse diaphragms is close to the secondary web. Compared with the current production of symmetrical layout structure, this layout provides a new idea for the design of stiffeners in the bias-rail box girder.

1. Introduction

Bias-rail box girder is a kind of box structure which is widely used. In most box girders made of thin plates, webs are slender and tend to buckle locally prior to flexural–torsional, distortional buckling or yielding under the action of bending-torsion. It leads to local instability and fatigue cracks. Eventually, it reduces the strength of the plates and leads to premature failure (Roberts and Davies, 2002; Alinia et al., 2007; Alinia and Moosavi, 2008; Qin et al., 2018). This experience forces engineers to use stiffeners in order to prevent the web from local instability. While transverse diaphragms are generally designed with the intent of enhancing the shear resistance of plate girder, longitudinal stiffening ribs are generally proportioned to help control lateral deflection of the web in its flexural compression zone and, subsequently, increase plate girder bending strength by increasing bending compressive stresses (Alinia, 2004; Gaby et al., 2014; Abid et al., 2015; Gaby et al., 2016; Qin et al., 2016). The stiffeners should be set at the peak or trough of the maximum warpage of the plate to prevent the deformation of the plate, so as to improve the stability of the plate.

Optimization techniques are powerful tools for improving traditional structural designs. In many real applications, stiffened plates and shell structures have been widely applied to marine, aerospace, automotive and other industries because of their lightweight construction. Some researchers have studied the layout optimization of stiffeners of these structures. In the shipbuilding industry, Gerry et al. (2019) proposed the hybrid Genetic Algorithm (GA) technique, which combined a genetic algorithm and subsequent optimization method, they optimized the stiffened plate at the bottom, side, and deck of the ship and obtained a structure that was lighter than that of the existing design. Liu et al. (2018) proposed a two-stage optimization method for the conceptual design of stiffeners in a ship's prow. Firstly, the distribution of stiffeners was determined by topology optimization method, and then the sizes of the plate and stiffeners were optimized simultaneously to minimize the cost and weight. In the automobile industry, Zbigniew (2009) used a genetic algorithm to solve the problem of weight minimization of a high-speed passenger-vehicle catamaran structure with specific design variables as

CORRESPONDENCE Yixiao Qin 1983015@tyust.edu.cn College of Mechanical Engineering, Taiyuan University of Science and Technology, Taiyuan 030024, China

dimensions of the plate thickness, longitudinal stiffeners, transverse frames and spacing between longitudinal and transversal members. In the field of aerospace, thin-walled stiffened parts generally have the characteristics of complex and irregular structure geometry. Wang et al. (2011) used the subset method to design a new layout of stiffeners for an aircraft wing to make the stiffeners lighter than the originals. Zhang et al. (2009) proposed the geometric background grid method to optimize the design of plane structure and curved thin-walled structure with the objective of maximizing the structural stiffness.

In recent years, many researches have focused on finding the optimal geometry shape and position of stiffeners on the thin-plate structures based on the elastic stability theory of thin plate to improve structural buckling performance. Liu et al. (2015) proposed a parameter-free shape optimization method of stiffeners on thin-walled structures. The issue of nondifferentiability was avoided by using the Kreisselmeier-Steinhauser function to transform the local objective functional into the smooth differentiable integral functional. Herencia et al. (2007) and Lee et al. (2002) optimized the shape of the T-shaped and I-shaped stiffeners on the thin plate respectively and obtained the optimal shape of the stiffeners under different loads. In addition, to obtain better buckling resistance, the optimum layout of stiffeners on the thin-walled plate and shell structure was of critical significance. Lee et al. (2004) proposed a geometry constraint-handling technique, which could define both convex and concave feasible stiffeners positioning regions and measure a degree of geometry constraint violation. This technique was applied to raise the first natural frequency of the thin-plate structure in the stiffeners layout optimization problem. Wang et al. (2003) optimized the layout of the stiffening plate with thermal residual stresses and determined the optimal location of these stiffeners to maximize the first natural frequency of the stiffened plate. Chen et al. (2019) used an improved gradient based two-level approximation (GA TA) to deal with the simultaneous optimization of stiffened shells with respect to distribution and sizes. Chen and Yang (2005) introduced the element sensitivity of the strain energy of stiffeners and presented a search criterion for location of stiffeners to identify the element efficiency so that most inefficiently used elements of stiffeners could be removed. Wang and Li (2018) and Li et al. (2016) took the element sensitivity information as the criterion for the layout of stiffeners and aimed at maximizing the stiffness of the structure to obtain the optimal position of stiffeners effectively. Wang et al. (2015) proposed an efficient and simple hybrid framework structure and optimized the numbers of stiffeners in plates subjected to the shear loading, which played the vital role in design of such structure. Vu et al. (2019) presented an investigation of the optimum location of multiple longitudinal web stiffeners for steel plates under pure bending by using the gradient-based interior point optimization algorithm, and the proposed formulas for determining the minimum rigidity requirement of the stiffeners were recommended for practical design purposes. Thang et al. (2009) carried out lightweight design of box girder with closed rectangular and open trapezoidal sections, and they determined the optimum cost design of changing thickness of continuous beam over equal span and the relationship between cross-section dimensions of steel box girders. Dong et al. (2020) optimized the perforated stiffened plate structure under unilateral axial pressure and shear loading based on the growth mechanism of branch systems in nature, and the buckling resistance performance of the optimized stiffened structure was greatly improved.

At present, the bias-rail box girder on the market uses symmetrical layout of longitudinal stiffening ribs and transverse diaphragms, and few studies conducted to optimize the sizes and layout of the stiffeners in the box girder. Based on the analysis and optimization of the layout and shape sizes of the stiffeners on the thin-plate structure by some researchers and the special structure of the bias-rail box girder, the optimum sizes and layout of longitudinal stiffening ribs and transverse diaphragms are obtained by taking a heavy-duty thin-plate box grideras an example. This asymmetric layout of stiffeners provides a new method for the structural design of the bias-rail box girder.

2. Layout Optimization Algorithm

2.1 Thin-Plate Box Grider

The layout of the internal stiffeners in complex thin-plate box grider is shown in Fig. 1.

The design variables which proposed in this study are shown in Fig. 2.

2.2 Intelligent Optimization Algorithm

2.2.1 Mathematical Model

The basic principle of the optimization problem is to establish a

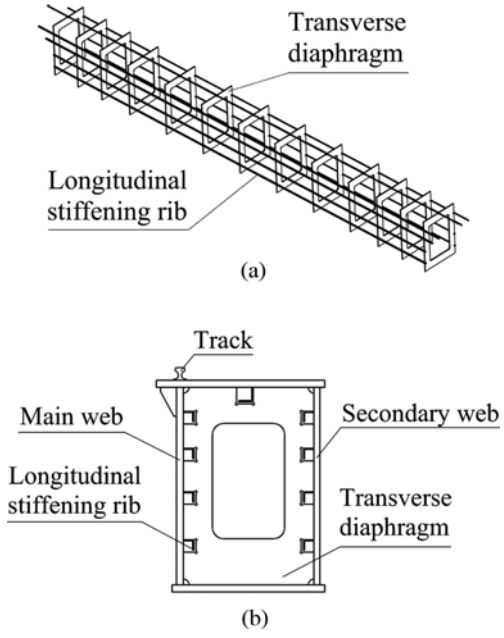

Fig. 1. Layout of Stiffeners in Bias-Rail Box Girder: (a) Internal Structure, (b) Cross Section

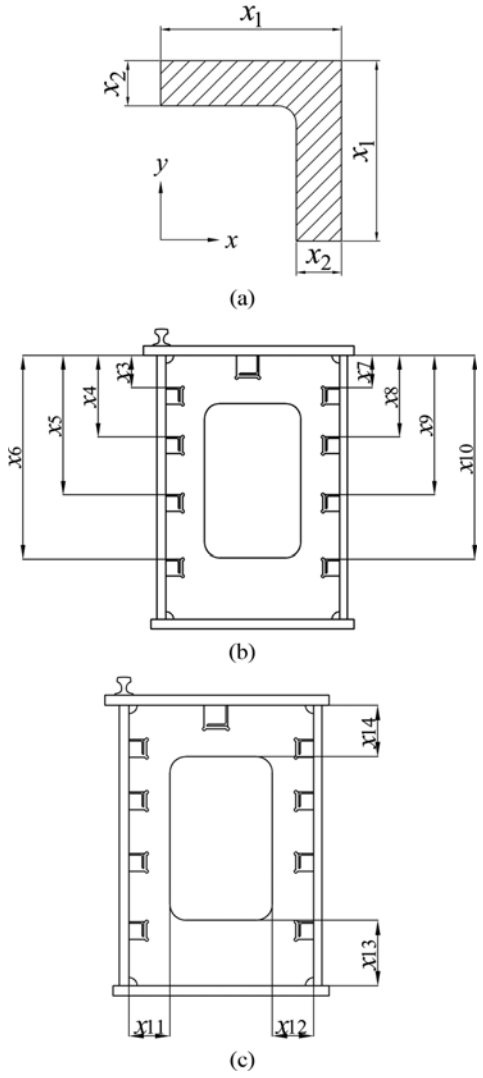

Fig. 2. Design Variables of Stiffeners in Bias-Rail Box Girder: (a) Sizes of Longitudinal Stiffening Ribs, (b) Location of Longitudinal Stiffening Ribs, (c) Hole Position of Transverse Diaphragms

mathematical model, under certain constraints, design variables are selected to obtain the optimal value of the objective function.

The mathematical model could be expressed as

$$\begin{aligned} &\min f(\boldsymbol{x}) \\ &\text{s.t.}\begin{cases} g_u(\boldsymbol{x}) \le 0 & u = 1,2,\cdots,m \\ h_v(\boldsymbol{x}) = 0 & v = 1,2,\cdots,p \end{cases} \\ &\boldsymbol{x} = [x_1, x_2, \cdots, x_n]^{\mathrm{T}}, \end{aligned} \tag{1}$$

where $f(x)$ is objective function, $g_u(x)$, $h_v(x)$ are constraint conditions, $\boldsymbol{x}$ is design vector.

2.2.2 Primary Function Approaching Method

The function approaching method is also called zero-order optimization method, it is essentially the least square approximation principle and characterized by the approaching of constraint conditions and objective function. Firstly, the approximations of the objective function and constraint conditions are obtained by random search. And the approximation curves of the objective function and constraint conditions are obtained by linear fitting, square fitting or square difference fitting. The Eq. (2) is approximate form of the objective function, including quadratic term and cross term. After approximating the objective function and constraint conditions, and then the constraint problem is transformed into an unconstrained problem by penalty function method, the form of Eq. (3) could be obtained:

$$f(\boldsymbol{x}) = a_0 + \sum_{i=1}^{n} a_i x_i + \sum_{i=1}^{n}\sum_{j=1}^{n} b_{ij} x_i x_j , \tag{2}$$

$$F(\boldsymbol{x}, q_k) = f(\boldsymbol{x}) + f_0 q_k \left(\sum_{i=1}^{n} P_x(x_i) + \sum_{u=1}^{m} P_g(g_u) + \sum_{v=1}^{p} P_h(h_v)\right), \tag{3}$$

where $P_x(x_i)$ is penalty function for design variables, $P_g(g_u)$ and $P_h(h_v)$ are penalty functions for constraint conditions, k is iteration index number, f_0 is the value of refering the objective function, it is used to adjust the ratio between functions, q_k is the response surface parameter of the introduced optimization function, which could improve the optimization precision.

The convergence criterion and equation is as follows:

1. The variation of the objective function between two adjacent designs should be less than the tolerance of objective function.
2. The variation of the objective function between the best reasonable design and the current design should be less than the tolerance of objective function.
3. The variation of the design variable between two adjacent designs should be less than the tolerance of design variables.
4. The variation of the design variable between the best reasonable design and the current design should be less than the tolerance of design variables.

$$\begin{cases} \left|f^{(j)} - f^{(j-1)}\right| \le \delta_f \\ \left|f^{(j)} - f^{(b)}\right| \le \delta_f \\ \left|x_i^{(j)} - x^{(j-1)}\right| \le \delta_x \\ \left|x_i^{(j)} - x^{(b)}\right| \le \delta_x \end{cases} \quad i = 1,2.3,\cdots,n \tag{4}$$

where δ_f is the tolerance of objective function and δ_x is the tolerance of design variables.

2.2.3 Latter Gradient Search Method

Gradient search method is also called first-order optimization method. It is characterized by partial derivative approximation of objective function and constraint conditions. The penalty function method is adopted to transform the constraint problem into the unconstrained problem, and the form of Eq. (5) could be obtained:

$$F(\boldsymbol{x}, q_k) = \frac{f(\boldsymbol{x})}{f_0} + q_k \left(\sum_{i=1}^{n} P_x(x_i) + \sum_{u=1}^{m} P_g(g_u) + \sum_{v=1}^{p} P_h(h_v)\right). \tag{5}$$

The unconstrained objective function $F(\boldsymbol{x}, q_k)$ is divided into objective function $F_f(\boldsymbol{x})$ and penalty function $F_q(\boldsymbol{x}, q_k)$, and the

form of Eq. (6) could be obtained:

$$\begin{cases} F_f(\boldsymbol{x})=\dfrac{f(\boldsymbol{x})}{f_0} \\ F_q(\boldsymbol{x},q_k)=q_k(\sum_{i-1}^{n}P_x(x_i)+\sum_{u-1}^{m}P_g(g_u)+\sum_{v-1}^{p}P_h(h_v)) \end{cases}, \tag{6}$$

$$F(\boldsymbol{x},q_k)=F_f(\boldsymbol{x})+F_q(\boldsymbol{x},q_k), \tag{7}$$

where $F_f(\boldsymbol{x})$ and $F_q(\boldsymbol{x},q_k)$ are related to the objective function and penalty function respectively.

For each optimization iteration (j), a search vector $\boldsymbol{d}^{(j)}$ in one direction is defined. In the initial iteration $j=0$, the search method is the fastest descent method. The search direction of unconstrained objective function $F(\boldsymbol{x},q_k)$ is assumed to be negative gradient direction, and its iterative expression is

$$\begin{cases} \boldsymbol{x}^{(j+1)}=\boldsymbol{x}^{(j)}+\alpha^{(j)}\boldsymbol{d}^{(j)} \\ \boldsymbol{d}^{(0)}=-\nabla F(\boldsymbol{x}^{(0)},q)=\boldsymbol{d}_f^{(0)}+\boldsymbol{d}_q^{(0)} \end{cases}, \tag{8}$$

where $\alpha^{(j)}$ is the smallest step of $F(\boldsymbol{x},q_k)$ in the $\boldsymbol{d}^{(j)}$ direction.

Then the conjugate direction method is used for calculation. $\boldsymbol{d}^{(j-1)}$ is expressed as linear combination of $\boldsymbol{d}^{(j)}$ and $-\nabla F(x^{(j)},q_k)$, and the modified formula of conjugate direction is obtained:

$$\boldsymbol{d}^{(j)}=-\nabla F(\boldsymbol{x}^{(j)},q_k)+\beta^{(j-1)}\boldsymbol{d}^{(j-1)}, \tag{9}$$

where $\beta^{(j-1)}$ is conjugate gradient parameter.

The convergence criterion and equation is as follows:

1. The variation of the objective function between two adjacent designs should be less than the tolerance of objective function.
2. The variation of the objective function between the best reasonable design and the current design should be less than the tolerance of objective function.

$$\begin{cases} \left|f^{(j)}-f^{(j-1)}\right|\le\delta_f \\ \left|f^{(j)}-f^{(b)}\right|\le\delta_f \end{cases}, \tag{10}$$

where δ_f is the tolerance of objective function.

2.2.4 Intelligent Optimization Algorithm Flow

The function approaching method is a coarse optimization method with a wide range of applicability, which is not easy to fall into the local extremum, but its optimization precision is not very high. While the gradient search method is a fine optimization method of local optimization with high precision, but it is easy to fall into the local extremum. The function approaching method and gradient search method are combined and improved in view of the shortcomings of them. Firstly, according to the least square approximation principle, a functional surface is selected to fit the solution space. The zero-order algorithm is used to determine the basic position of the optimal solution, and then the restart of optimal design is performed. The penalty function is added to the objective function to transform constraint problem into the unconstrained problem. Finally, the first-order algorithm based on gradient research optimization is used to modify the optimal solution, and then the precise optimal solution in the global sense is obtained, a high precision intelligent optimization algorithm is formed, and its flow chart is shown in Fig. 3.

3. Case Study

3.1 Modeling

The bias-rail box girder of heavy equipments is considered as the target model of this study. The outer layer of the box grider is box structure composed of the main web, secondary web and flange plates. There are numerous longitudinal stiffening ribs and transverse diaphragms in box girder, and the closed grider structure is formed. Its feature is that the rail is located above the main web, which effectively solves the problem of rail supporting. The overall configuration is shown in Fig. 4.

The material properties and element types of the modeling are shown in Table 1, and the parameterized finite element model of bias-rail box girder is obtained by Ansys.

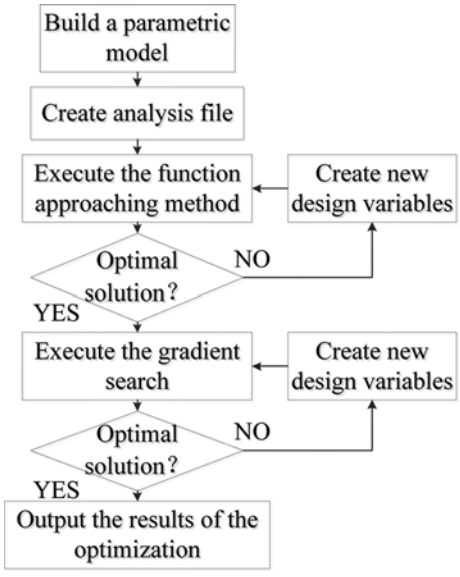

Fig. 3. Intelligent Optimization Algorithm Flow Chart

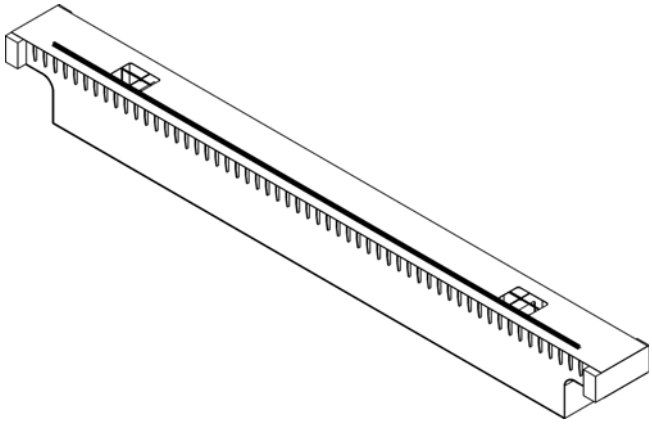

Fig. 4. The Overall Configuration of Bias-Rail Box Girder

Table 1. Material Properties and Element Types

Structure	Material	Elasticity modulus (MPa)	Poisson's ratio	Density (kg/m^3)	Element type
Longitudinal stiffening ribs	Q345	2.06E5	0.3	7,850	Shell63
Transverse diaphragms	Q345	2.06E5	0.3	7,850	Shell63
Webs and flange plates	Q345	2.06E5	0.3	7,850	Shell63
Track	U71Mn	2.06E5	0.3	7,850	Beam188

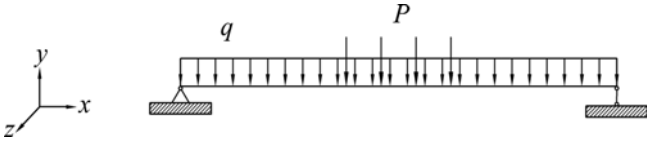

Fig. 5. Forces and Constraints

Table 2. Longitudinal Stiffening Ribs Type Descriptions

Longitudinal stiffening rib type	x_1 (mm)	x_2 (mm)	I_x (cm^4)
$L80\times$ 5	80	5	48.79
6		6	57.35
7		7	65.58
8		8	73.50
10		10	88.43
$L80\times$ 6	90	6	82.77
7		7	94.83
8		8	106.5
10		10	128.6
12		12	149.2
$L80\times$ 6	100	6	115
7		7	131
8		8	148.2
10		10	179.5
12		12	208.9
14		14	236.5
16		16	262.5
$L80\times$ 7	110	7	177.2
8		8	199.5
10		10	242.2
12		12	282.6
14		14	320.7

Bias-rail box girder is considered as simply supported beam. UX, UY and UZ translational degrees of freedom and ROTX and ROTY rotational degrees of freedom are applied on one side, while UY and UZ translational degrees of freedom and ROTX and ROTY rotational degrees of freedom are applied on the other side. When the fully loaded trolley about 450t is located in the middle of the span, the mechanical model that subjected to uniformly distributed gravity loads and concentrated forces is shown in Fig. 5.

3.2 Layout Optimization Design Variables

In this study, the type of the longitudinal stiffening ribs is considered as discrete design variables. The four possible types are shown in Table 2. The location of longitudinal stiffening ribs, the hole position and thickness of transverse diaphragms are considered as continuous design variables, they are shown in Fig. 2, the initial design and upper and lower limit are shown in Table 3.

Table 3. Design Variables Descriptions

Item	Initial design (mm)	Upper and lower limit (mm)
x_1	100	80,110
x_2	10	5,12
x_3	395	380,410
x_4	875	860,890
x_5	1570	1560,1580
x_6	2265	2255,2275
x_7	395	380,410
x_8	875	860,890
x_9	1570	1560,1580
x_{10}	2265	2255,2275
x_{11}	300	250,350
x_{12}	300	250,350
x_{13}	450	400,500
x_{14}	350	300,400
Transverse diaphragms thickness x_{15}	20	15,25

3.3 Constraint Conditions

Constraints are conditions which the optimization solution must satisfy. In this study, according to the design criteria of box grider, when the fully loaded trolley is located in the middle of the span, the midspan maximum stress σ_{max} and the midspan maximum deflection Y_{max} are constraint conditions. The midspan maximum stress σ_{max} = 131.01 MPa and the midspan maximum deflection Y_{max} = 21.21 mm are extracted by general post-processing module before optimization.

Strength constraint

$$g_1(\boldsymbol{x})=\sigma_{max}-[\sigma]=\sigma_{max}-\frac{0.5\sigma_s+0.35\sigma_b}{n}=\sigma_{max}-227.7\le 0 \quad (11)$$

where σ_s is yield strength of the material, σ_b is tensile strength of the material, n is safety factor, n = 1.48.

Stiffness constraint

$$g_2(\boldsymbol{x})=Y_{max}-[Y]=Y_{max}-\frac{28900}{1000}=Y_{max}-28.9\le 0 , \quad (12)$$

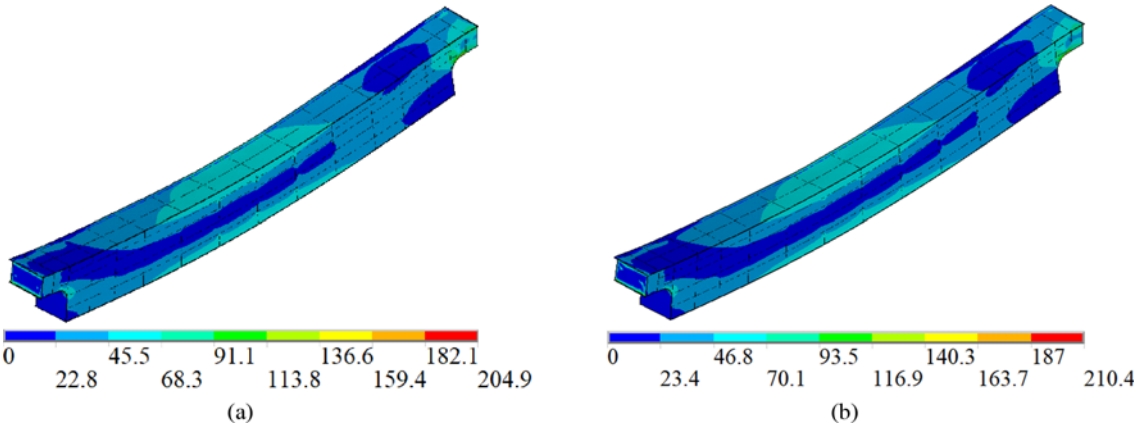

Fig. 6. Comparison of the Stress Distribution of Initial Design and Final Design: (a) Initial Design, (b) Final Design

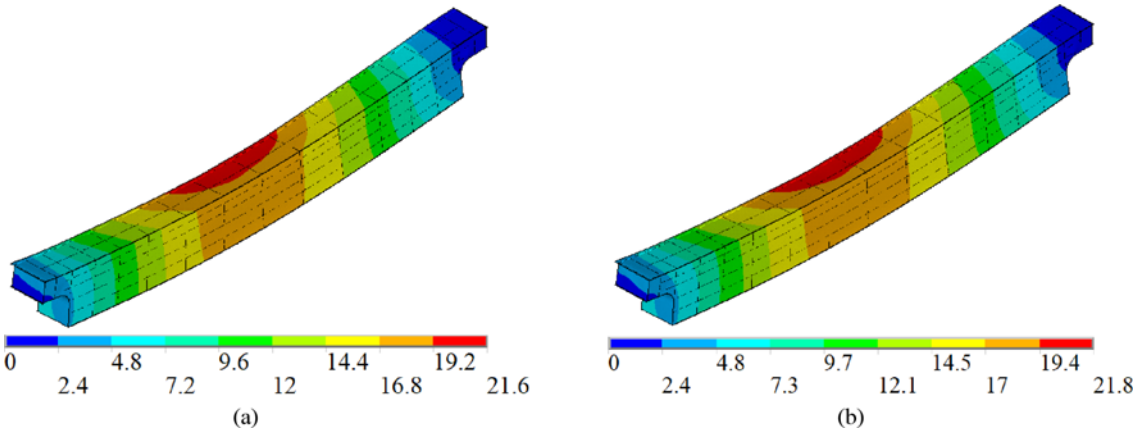

Fig. 7. Comparison of the Displacement Distribution of Initial Design and Final Design: (a) Initial Design, (b) Final Design

where Y_{max} is the maximum deflection of the box grider when the concentrated forces are in the middle of span, $[Y]$ is the allowable deflection of the box grider.

3.4 Objective Function

The objective function is a dependent variable that is hoped to minimize in the optimization. The ultimate goal of optimization in this study is to minimize the weight of longitudinal stiffening ribs and transverse diaphragms under the given conditions. For structural component with uniform density, it is to minimize its volume. Therefore, the total volume is selected as the objective function, and the total volume before optimization is extracted $v = 6.46 \times 10^9$ mm^3.

3.5 Optimization Results

By combining the function approaching method with the gradient optimization method, the section sizes and layout of longitudinal stiffening ribs and the hole position and thickness of transverse diaphragms are optimized. In the actual production and application, it is difficult to have decimal number in the structure sizes, so the sizes after optimization of the model are rounded up to the values shown in Table 4.

As the optimization results show, the sizes of longitudinal stiffening ribs and transverse diaphragms decreased. As for the discrete design variables of the longitudinal stiffening ribs, according to Tables 2 and 4, $L80 \times 5$ longitudinal stiffening rib is

Table 4. Optimization Results

Item	Initial design	Final design
x_1 (mm)	100	80
x_2 (mm)	10	5
x_3 (mm)	395	403
x_4 (mm)	875	866
x_5 (mm)	1,570	1,579
x_6 (mm)	2,265	2,274
x_7 (mm)	395	409
x_8 (mm)	875	888
x_9 (mm)	1,570	1,576
x_{10} (mm)	2,265	2,274
x_{11} (mm)	300	347
x_{12} (mm)	300	344
x_{13} (mm)	450	427
x_{14} (mm)	350	303
Transverse diaphragms thickness x_{15} (mm)	20	15
Midspan maximum deflection Y_{max} (mm)	21.21	21.38
Midspan maximum stress σ_{max} (MPa)	131.01	132.05
Total volume v (mm^3)	6.46×10^9	6.02×10^9

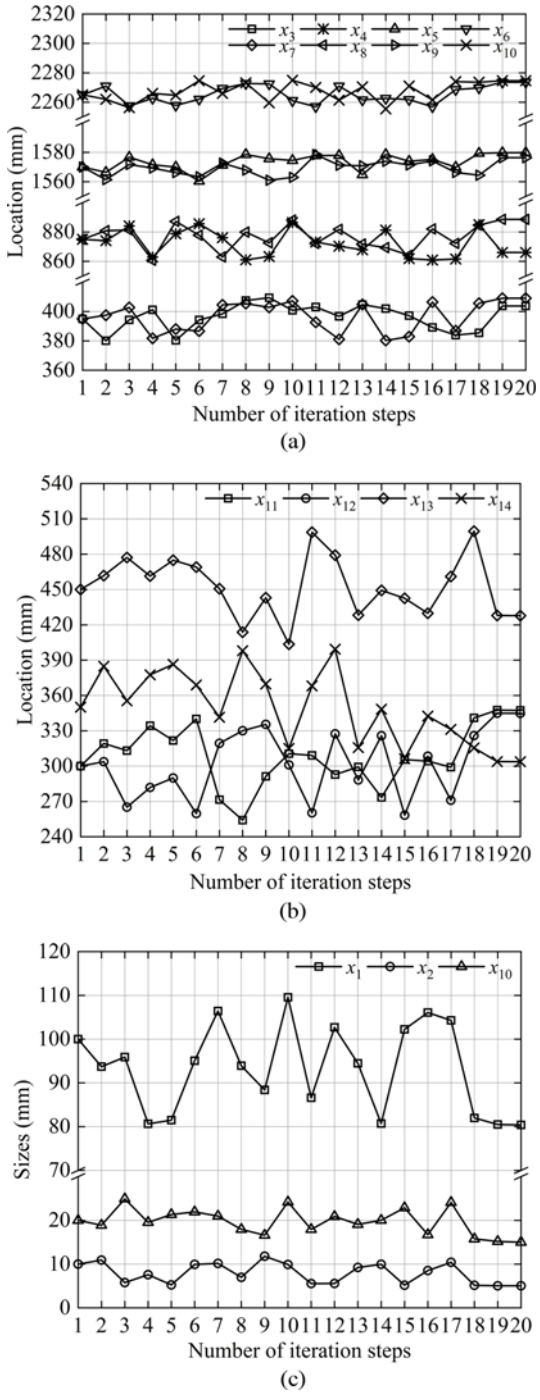

Fig. 8. Optimization Curves of Design Variables: (a) Layout of Longitudinal Stiffening Ribs, (b) Hole Position of Transverse Diaphragms, (c) Sizes

selected. The constraint conditions midspan maximum stress and midspan maximum deflection before optimization are σ_{max} = 131.01 MPa and Y_{max} = 21.21 mm, and after optimization, they are σ_{max} = 132.05 MPa and Y_{max} = 21.38 mm. They both get increased, but they are both in the allowable range. The objective function total volume v is 6.46×10^9 mm^3 before optimization and 6.02×10^9 mm^3 after optimization. Since the weight of the box grider is proportional to its volume, so its weight is reduced approximately $(6.46 \times 10^9 - 6.02 \times 10^9)/6.46 \times 10^9 \approx 7\%$. The

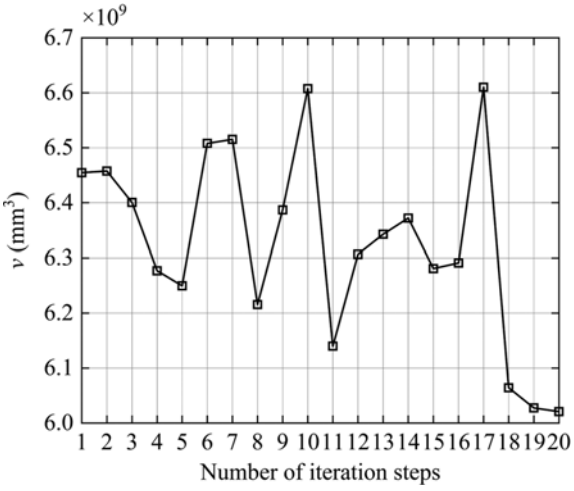

Fig. 9. Optimization Curve of Objective Function v

optimization effect is evident. The stress nephogram and displacement nephogram before and after optimization are shown in Figs. 6 and 7. Before optimization, the maximum stress is 204.9 MPa and the maximum strain is 21.6 mm. After optimization, the maximum stress is 210.4 MPa and the maximum strain is 21.8 mm, they get increased, but they are both in the allowable range. The optimal sizes and layout of longitudinal stiffening ribs and transverse diaphragms are obtained under the design requirements of strength and stiffness of the box grider.

The changes of design variables and objective function with iteration times in this optimization are shown in Figs. 8 and 9. It could be seen that the design variables and objective function have converged at the 20th iteration.

3.6 Results Analysis

The bending moment on the cross section of the bias-rail box girder is balanced by the bending normal stress. According to the bending moment on the grider section, the normal stress distribution could be further calculated. According to the assumption of planecross-section, there is a neutral layer in the box grider that the fiber length does not change before and after deformation. It divides the box grider into two parts: the upper part is subjected to compressive stress, the lower part is subjected to tensile stress. After bending and deformation, there is the following relationship between the radius of curvature ρ of a point on the deflection curve and the bending moment M on the section at that point:

$$\frac{1}{\rho} = \frac{M}{EI}, \tag{13}$$

where E is modulus of elasticity of material, I is the moment of inertia of the section towards the neutral layer, EI is the bending stiffness, which reflects the ability of the box grider to resist bending deformation. As shown in Fig. 10, the bending normal stress at any point on the cross section is proportional to the

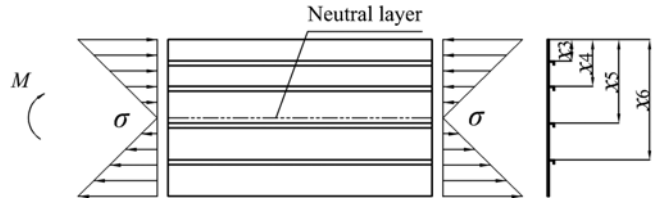

Fig. 10. Schematic Diagram of Bending Normal Stress Distribution

distance from this point to the neutral layer. The calculation formula of bending normal stress is as follows:

$$\sigma=\frac{My}{I}, \tag{14}$$

where σ is the normal stress at a point on the cross section, y is the distance from that point to the neutral layer.

According to the bending theory of the grider mentioned above, it could be seen from the comparison diagram of the layout of longitudinal stiffening ribs in Fig. 11, the point farther away from the neutral layer on the cross section has larger normal stress, so longitudinal stiffening ribs should be arranged as far away from the neutral layer as possible. Also, the loading environment on the main web is worse than that on the secondary web, the location of longitudinal stiffening ribs on the main web should be farther from the neutral layer than that on the secondary web. Similarly, it could be seen from the comparison diagram of the hole position of transverse diaphragms in Fig. 12. The hole position of transverse diaphragms should be close to the secondary web. This layout makes full use of the material and better bears the wheel pressure on the rail. It provides new method for the layout design of longitudinal stiffening ribs and transverse diaphragms in the box grider.

4. Conclusions

In this study, the bias-rail box girder of heavy equipments is considered as the target model. The function approaching method and the gradient search method are combined to form a high-precision comprehensive optimization algorithm. The longitudinal stiffening ribs and transverse diaphragms in box girder are designed with light weight, Finally the weight is reduced by nearly 7%. The optimized sizes could better meet the requirements

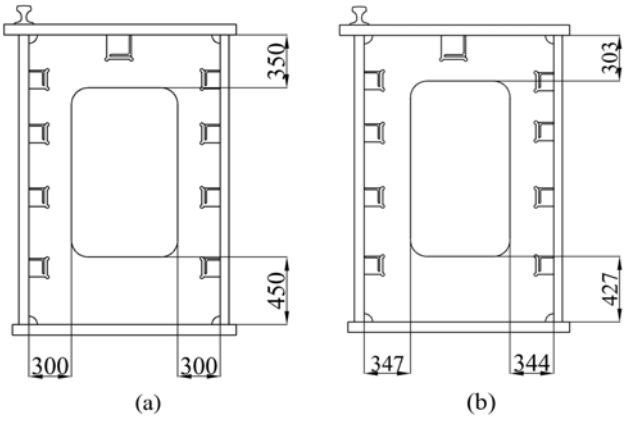

Fig. 12. Hole Position of the Transverse Diaphragms of Initial Design and Final Design: (a) Initial Design, (b) Final Design

of lightweight design and effectively reduce the weight of the structure and the manufacturing cost of the enterprises.

Further, the loading environment on the main web is worse than that on the secondary web because the trolley track is located above the main web. Therefore, according to the optimization results and Fig. 10, in the design of the bias-rail box girder, the distance between the longitudinal stiffening ribs on the main web and the neutral layer should be longer than the distance between the longitudinal stiffening ribs on the secondary web and the neutral layer, and the hole position of transverse diaphragms should be close to the secondary web. Compared with the current production of symmetrical layout structure in the market, the use of asymmetrical layout of longitudinal stiffening ribs and hole position of transverse diaphragms could not only increase the bearing capacity of the structure, but also prevent local instability and fatigue cracks of the main web and the secondary web. This layput provides a new idea for the design of stiffeners in heavy-duty thin-plate box grider.

Acknowledgments

This research was supported by the National Key R&D Program of China (2017YFC0703906), the Shanxi Provincial Key Research and Development Project (201903D121067), the Fund for Shanxi '1331 Project' Key Subjects Construction (1331KSC).

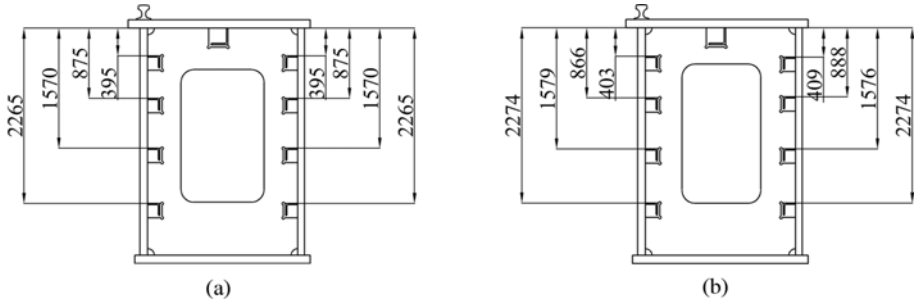

Fig. 11. Layout of Longitudinal Stiffening Ribs of Initial Design and Final Design: (a) Initial Design, (b) Final Design

ORCID

Not Applicable

References

Abid M, Akmal MH, Wajid HA (2015) Design optimization of box type girder of an overhead crane. *Iranian Journal of Science and Technology* 39(M1):101-112, DOI: 10.22099/IJSTM.2015.2952

Alinia MM (2004) A study into optimization of stiffeners in plates subjected to shear loading. *Thin-Walled Structures* 43(5):845-860, DOI: 10.1016/j.tws.2004.10.008

Alinia MM, Hosseinzadeh SAA, Habashi HR (2007) Influence of central cracks on buckling and post-buckling behaviour of shear panels. *Thin-Walled Structures* 45(4):422-431, DOI: 10.1016/j.tws.2007.03.003

Alinia MM, Moosavi SH (2008) A parametric study on the longitudinal stiffeners of web panels. *Thin-Walled Structures* 46(11):1213-1223, DOI: 10.1016/j.tws.2008.02.004

Chen SY, Dong TS, Shui XF (2019) Simultaneous distribution and sizing optimization for stiffeners with an improved genetic algorithm with two-level approximation. *Engineering Optimization* 51(11): 1845-1866, DOI: 10.1080/0305215X.2018.1558444

Chen SH, Yang ZJ (2005) The layout optimization of stiffeners for plate-shell structures. *Acta Mechanica Solida Sinica* 18(4):365-373

Dong XH, Ding XH, Li GJ, Lewis GP (2020) Stiffener layout optimization of plate and shell structures for buckling problem by adaptive growth method. *Structural and Multidisciplinary Optimization* 61(5):301-318, DOI: 10.1007/s00158-019-02361-0

Gaby IEK, Daniel GL, Louis FG (2014) Computational studies of horizontally curved, longitudinally stiffened, plate girder webs in flexure. *Journal of Constructional Steel Research* 93:93-106, DOI: 10.1016/j.jcsr.2013.10.018

Gaby IEK, Daniel GL, Louis FG (2016) Flexure–shear interaction influence on curved, plate girder web longitudinal stiffener placement. *Journal of Constructional Steel Research* 120:97-106, DOI: 10.1016/j.jcsr.2015.12.021

Gerry LP, Mitsuru K, Akihiro T (2019) Structural optimization of stiffener layout for stiffened plate using hybrid GA. *International Journal of Naval Architecture and Ocean Engineering* 11(2):809-818, DOI: 10.1016/j.ijnaoe.2019.03.005

Herencia JE, Weaver PM, Friswell MI (2007) Initial sizing optimisation of anisotropic composite panels with T-shaped stiffeners. *Thin-Walled Structures* 46(4):399-412, DOI: 10.1016/j.tws.2007.09.003

Lee JH, Kim GH, Park YS (2004) A geometry constraint handling technique for stiffener layout optimization problem. *Journal of Sound and Vibration* 285(1):101-120, DOI: 10.1016/j.jsv.2004.08.010

Lee GR, Yang WH, Suh MW (2002) Optimum shape for buckling and post-buckling behavior of a laminated composite panel with I-type stiffeners. *Journal of Mechanical Science and Technology* 16(10):1211-1221, DOI: 10.1007/BF02983827

Li L, Zhang B, Li CQ, Tan SN (2016) Stiffener layout optimization of thin plate structures based on sensitivity number. *China Mechanical Engineering* 27(09):1143-1149, DOI: 10.3969/j.issn.1004-132X.2016.09.002

Liu ZJ, Cho SG, Takezawa A, Zhang XP, Kitamura M (2018) Two-stage layout–size optimization method for prow stiffeners. *International Journal of Naval Architecture and Ocean Engineering* 11:44-51, DOI: 10.1016/j.ijnaoe.2018.01.001

Liu Y, Shimoda M, Shibutani Y (2015) Parameter-free method for the shape optimization of stiffeners on thin-walled structures to minimize stress concentration. *Journal of Mechanical Science and Technology* 29(4):1383-1390, DOI: 10.1007/s12206-015-0308-6

Qin YX, Li BL, Li X, Li YQ, Zhang ZD, Gu CY, Gu HZ (2018) Vibration analysis and control of nuclear power crane with MRFD. *International Journal of Applied Mechanics* 10(8):1850093, DOI: 10.1142/S175882511850093X

Qin YX, Xie WT, Ren HP, Li X (2016) Crane hook stress analysis upon boundary interpolated reproducing kernel particle method. *Engineering Analysis with Boundary Elements* 63:74-81, DOI: 10.1016/j.enganabound.2015.11.006

Roberts TM, Davies AW (2002) Fatigue induced by plate breathing. *Journal of Constructional Steel Research* 58(12):1495-1508, DOI: 10.1016/S0143-974X(02)00008-1

Thang DD, Koo MS, Hameed A (2009) Optimum cost design of steel box-girder by varying plate thickness. *KSCE Journal of Civil Engineering* 13(1):31-37, DOI: 10.1007/s12205-009-0031-x

Vu QV, Truong VH, George P, Carlos G, Kim SE (2019) Bend-buckling strength of steel plates with multiple longitudinal stiffeners. *Journal of Constructional Steel Research* 158:41-52, DOI: 10.1016/j.jcsr.2019.03.006

Wang XM, Hansen JS, Oguamanam DCD (2003) Layout optimization of stiffeners in stiffened composite plates with thermal residual stresses. *Finite Elements in Analysis and Design* 40(9):1233-1257, DOI: 10.1016/j.finel.2003.06.003

Wang D, Li ZH (2018) Layout optimization method for stiffeners of plate structure. *Chinese Journal of Computational Mechanics* 35(02): 138-143, DOI: 10.7511/jslx20161229001

Wang Q, Lu ZZ, Zhou CC (2011) New topology optimization method for wing leading-edge ribs. *Journal of Aircraft* 48(5):1741-1748, DOI: 10.2514/1.C031362

Wang B, Tian K, Hao P, Cai YW, Li YW, Sun Y (2015) Hybrid analysis and optimization of hierarchical stiffened plates based on asymptotic homogenization method. *Composite Structures* 132:136-147, DOI: 10.1016/j.compstruct.2015.05.012

Zbigniew S (2009) Least-weight topology and size optimization of high speed vehicle-passenger catamaran structure by genetic algorithm. *Marine Structures* 22(4):691-711, DOI: 10.1016/j.marstruc.2009.06.003

Zhang WH, Zhang SD, Gao T (2009) Stiffener layout optimization of thin-walled structures. *Acta Aeronautica et Astronautica Sinica* 30(11):2126-2131, DOI: 10.3321/j.issn:1000-6893.2009.11.018